Macromolecules

pubs.acs.org/Macromolecules | Article

2-(Benzylthio)ethyl Glycidyl Ether: A Gateway to Redox-Responsive Polyethers

Ahyun Kim, Jinsu Baek, and Byeong-Su Kim*

Cite This: https://doi.org/10.1021/acs.macromol.4c00949 | Read Online

ACCESS | Metrics & More | Article Recommendations | Supporting Information

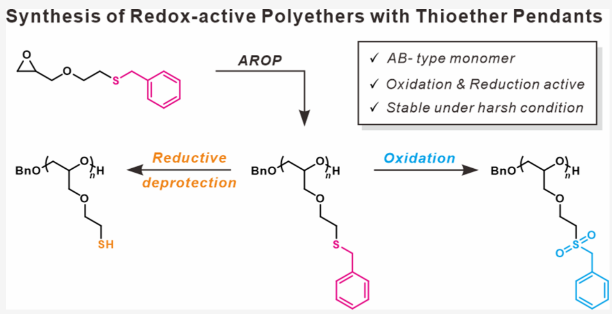

ABSTRACT: This work presents the design and synthesis of a functional epoxide monomer, 2-(benzylthio)ethyl glycidyl ether (BTGE), serving as a versatile building block for the development of redox-responsive polyethers. It details the successful synthesis of a series of poly(2-(benzylthio)ethyl glycidyl ether) (PBTGE) homopolymers and ABA-type triblock copolymers (i.e., PBTGE-*b*-PEO-*b*-PBTGE), achieved through controlled anionic ring-opening polymerization of the BTGE using a poly(ethylene oxide) (PEO) macroinitiator. Comprehensive characterization of the synthesized monomers and polymers was performed employing various analytical techniques, such as ^{1}H- and ^{13}C NMR, GPC, FT-IR spectroscopy, and MALDI-ToF mass spectrometry. These polymers demonstrate unique redox-responsive behavior, characterized by an oxidation-induced transition from hydrophobic to hydrophilic states and a reductive deprotection to generate free thiol groups. Furthermore, the PBTGE-*b*-PEO-*b*-PBTGE triblock copolymers have been utilized to form physically cross-linked hydrogels through the strong hydrophobic interactions of the end blocks. Notably, these hydrogels undergo a gel-to-sol transition under oxidative conditions, as evidenced by rheological analysis. This study highlights the potential of the BTGE monomer as a versatile building block for the development of advanced materials with dual redox-responsive functionalities.

■ INTRODUCTION

Biomaterials, encompassing both natural and synthetic forms, have become essential in modern medicine for restoring the physiological functions of soft tissues, organs, and bones and enabling the controlled release of therapeutic agents.[1] A pivotal advancement in this domain has been the development of stimuli-responsive polymers, engineered to change their physical and/or chemical properties in response to environmental stimuli such as pH,[2] mechanical force,[3] temperature,[4] enzyme activity,[5] or redox balance.[6,7] These polymers are promising for drug/gene delivery, tissue engineering, and biosensors.[8−10]

Redox-responsive polymers, in particular, have garnered attention due to their ability to respond to changes in the redox environment of cells and tissues under pathological conditions such as cancer, inflammation, and wound healing.[11,12] For example, polymers with disulfide bond side chains can undergo reduction to their corresponding thiols in the reducing potential of the intracellular environment primarily driven by the higher concentration of glutathione (GSH) in the cytosol (reaching as high as 10 mM) compared to extracellular fluids (2−10 μM). Conversely, disulfides remain stable in oxidative conditions due to the higher concentration of cystine relative to cysteine and reduced GSH.[13]

Furthermore, reactive oxygen species (ROS) are formed from incomplete oxygen reduction, which play a crucial role in regulating various physiological functions. However, excessive ROS production can cause oxidative stress, leading to several diseases. To date, a considerable body of research has thus focused on developing biomaterials that leverage the unique characteristics of ROS for therapeutic interventions[14,15] For instance, ROS-responsive systems incorporating thioether,[16] thioketal,[17] selenide,[18] diselenide,[19] arylboronic ester,[20] or oligoproline[21] moieties have been designed to mitigate inflammatory diseases by modulating ROS levels and reducing the side effects of conventional treatments like corticosteroids.[22] Conventionally, oxidation reactions involving these ROS-sensitive moieties either induce a change in solubility by facilitating a transition from hydrophobic to hydrophilic states or lead to the reduction-induced cleavage of prodrugs and linkers[23,24] For example, Gu et al. engineered a ROS-responsive PEG-based hydrogel with L-methionine for

Received: April 25, 2024
Revised: August 14, 2024
Accepted: August 19, 2024

Scheme 1. (a) Illustration of Redox-Active Monomers with Distinct Characteristics;[27,28] (b) Synthetic Procedure for BTGE Monomer; (c) Polymerization of Thioether (PBTGE) and Its Redox-Responsive Properties Leading to Sulfone (PBSGE) and Free Thiol (PTGE); (d) Preparation of Triblock Copolymers and Hydrogels Featuring Oxidation-Triggered Disassembly Mechanism

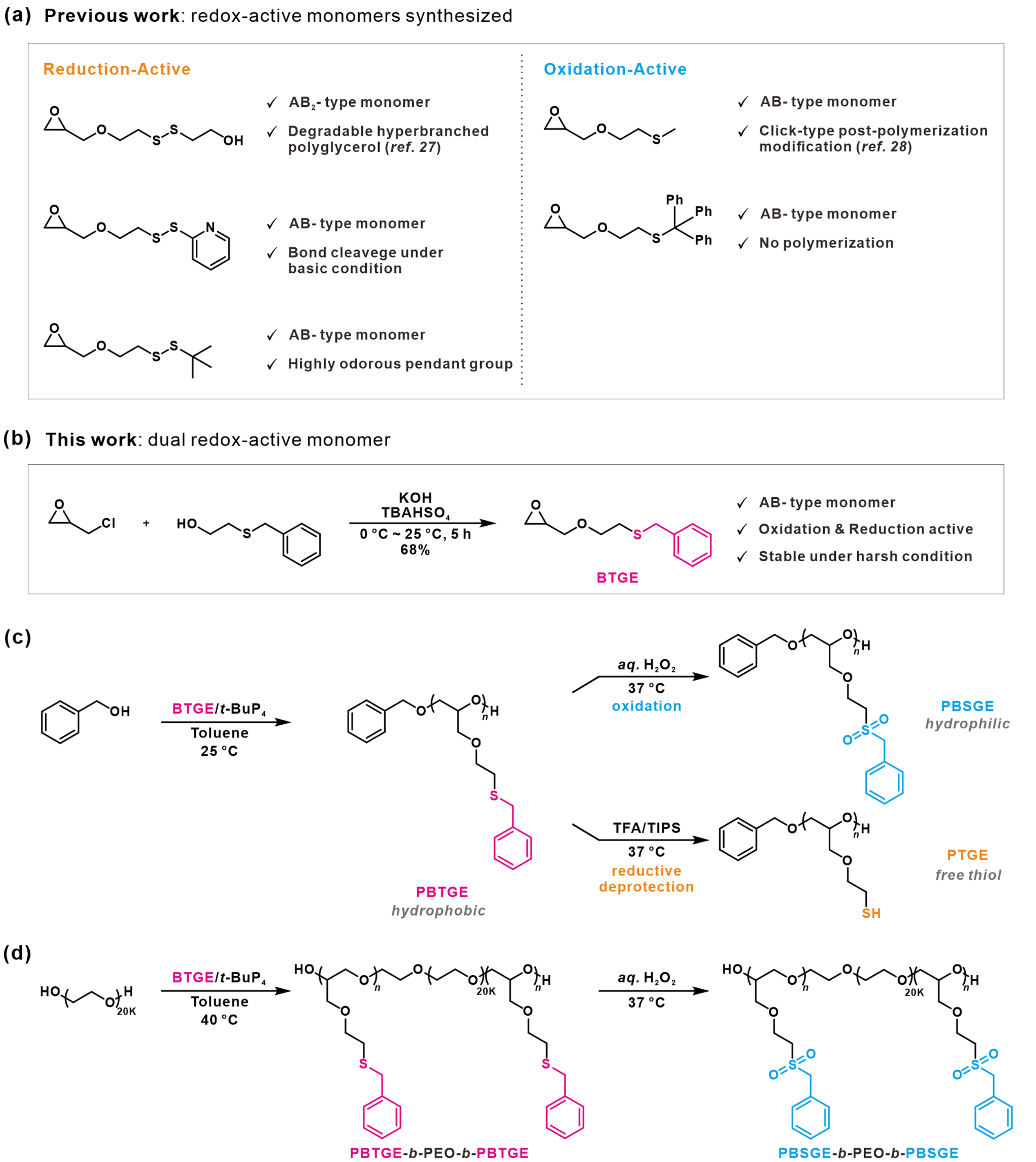

drug release, showcasing a solubility shift from hydrophobic thioether to hydrophilic sulfoxide and sulfone. This hydrogel served as a targeted drug delivery system and modulated the intratumoral microenvironment to enhance therapeutic efficacy.[25] Meanwhile, Kim et al. devised an activatable prodrug that uses the cleavage of the boronate ester induced by physiological levels of H_2O_2 to trigger the activation of a fluorophore for metastatic tumor treatment. This dual-functionality not only enabled the sensitive tumor detection, but also facilitated the targeted chemotherapeutic agent delivery.[26]

In our continuous pursuit of novel functional epoxide monomers, we previously introduced a reduction-responsive glycidyl ether, 2-((2-(oxiran-2-ylmethoxy)ethyl) disulfanyl)-

https://doi.org/10.1021/acs.macromol.4c00949
Macromolecules XXXX, XXX, XXX−XXX

ethan-1-ol.[27] Concurrently, Frey and coworkers reported the synthesis of an oxidation-responsive monomer, 2-(methylthio)ethyl glycidyl ether, and its application to the responsive micelles.[28] The versatility of this monomer was demonstrated by incorporating a clickable sulfonium group through alkylation/alkoxylation reactions. Initially, our efforts focused on the synthesis of the redox-active functional epoxide monomers (Scheme 1a and Figure S1). However, challenges arose with each functional group. For instance, a pyridyl disulfide bond cleavage was observed in the presence of water and base during Williamson ether synthesis, thereby prompting us to substitute it with chemically stable *t*-butyl mercaptan. While *t*-butyl mercaptan improved stability, it also presented issues such as malodor and a low boiling point. Additionally, the attempt to enhance the stability of hydrophobic drugs by incorporating a trityl moiety into an epoxide monomer resulted in poor solubility and negligible initiation efficiency in anionic ring-opening polymerization and Lewis-pair polymerization. Therefore, the development of a monomer capable of withstanding harsh reaction conditions, while encompassing both reduction and oxidation characteristics, became highly desirable.

Herein, we introduce a versatile epoxide monomer, 2-(benzylthio)ethyl glycidyl ether (BTGE), featuring a thioether group that serves both as a protecting group for thiols and a redox-responsive functional group (Scheme 1b). An array of various poly(2-(benzylthio)ethyl glycidyl ether) (PBTGE) homopolymers and ABA-type triblock copolymers of PBTGE-*b*-PEO-*b*-PBTGE are synthesized through controlled anionic ring-opening polymerization using a poly(ethylene oxide) (PEO) macroinitiator (Scheme 1c). The triblock copolymer hydrogels are self-assembled via robust hydrophobic interactions of the BTGE end-blocks in an aqueous environment (Scheme 1d). These hydrogels were subsequently disassembled into solution upon an oxidation-induced hydrophobic-to-hydrophilic transition. This innovative approach addresses the challenges encountered in aforementioned attempts and lays a solid foundation for developing redox-responsive materials for biomedical applications.

■ EXPERIMENTAL SECTION

Materials. 2-(Benzylthio)ethanol (>98.0%) and epichlorohydrin (>99.0%) were purchased from Tokyo Chemical Industry. Benzyl alcohol (99.8%), phosphazene base *t*-BuP$_4$ solution (0.80 M in hexane), tetrabutylammonium hydrogensulfate (97%), potassium hydroxide, toluene and Nile Red were obtained from Sigma-Aldrich. All chemicals were used as received unless noted otherwise. The BTGE monomer and toluene were dried over CaH_2 and freshly distilled before polymerization. Deuterated NMR solvent CD_2Cl_2 was obtained from Cambridge Isotope Laboratories.

Characterizations. ^{1}H, ^{13}C, COSY, and HSQC NMR spectra were recorded at room temperature on a Bruker Avance II 400 MHz spectrometer. Chemical shifts are reported in ppm relative to the residual solvent peaks: CD_2Cl_2, δH = 5.32 ppm, and δC = 54.00 ppm. Mass spectrometry was performed using a Waters Xevo G2-XS time-of-flight (ToF) instrument with an electrospray ionization (ESI) source. Gel permeation chromatography (GPC) analyses were carried out with tetrahydrofuran (THF) as an eluent at 25 °C and a flow rate of 1.0 mL min^{-1} employing an Agilent 1200 Series system with an autoinjector and a refractive index (RI) detector. The number- and weight-averaged molecular weights (M_n and M_w) and polydispersity index (M_w/M_n, $Đ$) were determined using polystyrene (PS) standards (Sigma-Aldrich; M_p, 250–1,100,000 g mol^{-1}). Matrix-assisted laser desorption and ionization-time-of-flight (MALDI-ToF) mass spectrometry was conducted on a Bruker Autoflex Max. Fourier-transform infrared (FT-IR) spectra were collected using an Agilent Cary 630 spectrometer equipped with an attenuated total reflection (ATR) module. Differential scanning calorimetry (DSC) analyses were performed under nitrogen, from −80 to 100 °C, with a heating and cooling rate of 10 °C min^{-1} on a TA Instruments Q200 model. Raman spectrum was collected via Horiba LabRam Aramis (532 nm, 40x magnification). Model dye release test was carried out via using a Shimadzu RF-6000 spectrofluorophotometer.

Synthesis of BTGE Monomer. A 40% KOH aqueous solution was prepared by dissolving 18.67 g of potassium hydroxide in 28.00 mL of water in a 100 mL round-bottom flask. Tetrabutylammonium hydrogensulfate (0.57 g, 1.66 mmol) was added, and the mixture was stirred for 30 min in an ice bath. Then, epichlorohydrin (13 mL, 166.4 mmol) and 2-(benzylthio)ethanol (5.6 g, 33.28 mmol) were slowly added with a dropping funnel. The reaction was monitored by thin-layer chromatography and conducted for 5 h at 25 °C. The crude product was extracted with ethyl acetate, washed with brine, dried over Na_2SO_4, and concentrated in vacuo. The crude was purified by column chromatography (ethyl acetate/hexane = 1:7) yielded a colorless oil, which was further distilled over CaH_2 (5.08 g, 22.63 mmol, 68.0% yield). ^{1}H NMR (400 MHz, CD_2Cl_2): δ 7.43–7.15 (m, 5H), 3.80–3.69 (m, 3H), 3.66–3.54 (m, 2H), 3.29 (dd, J = 11.5, 6.2 Hz, 1H), 3.09 (ddt, J = 6.2, 4.1, 2.7 Hz, 1H), 2.75 (dd, J = 5.0, 4.3 Hz, 1H), 2.61 (t, J = 6.7 Hz, 2H), 2.55 (dd, J = 5.0, 2.7 Hz, 1H). ^{13}C NMR (101 MHz, CD_2Cl_2): δ 139.20, 129.43, 128.94, 127.44, 72.28, 71.36, 51.15, 44.43, 37.03, 31.27. Electrospray ionization mass spectrometry (ESI-MS) (m/z): [M + Na]$^+$ calcd 247.08; obs. 246.90.

Synthetic Procedure for PBTGE Homopolymers. Under an argon atmosphere in a glovebox, a benzyl alcohol solution (10.4 μL, 0.10 mmol, 1.0 equiv) in anhydrous toluene (1.0 M, 0.65 mL) was prepared. To this solution, 125 μL of a *t*-BuP$_4$ solution (0.8 M in hexane, 0.10 mmol, 1.0 equiv) was added and stirred for 30 min. The polymerization was initiated by adding BTGE (224.09 mg, 1.00 mmol, 10 equiv) dropwise, and the reaction was monitored by ^{1}H NMR. After stirring at room temperature for 1 h, the polymerization was quenched with an excess amount of methanol. The mixture was then passed through an alumina pad using dichloromethane (DCM), and the solvent was evaporated to yield PBTGE. ^{1}H NMR (400 MHz, CD_2Cl_2): δ 7.39–7.15 (m, 50H), 3.71 (s, 20H), 3.66–3.33 (m, 70H), 2.55 (t, J = 6.7 Hz, 20H). ^{13}C NMR (101 MHz, CD_2Cl_2): δ 139.25, 129.46–128.98, 127.46, 79.32, 71.52, 70.30, 37.09, 31.40. $Đ$ (GPC, THF, PS standard) = 1.11.

Oxidation of PBTGE Homopolymers. Herein, 60 mg of PBTGE$_{10}$ (0.25 mmol of the thioether functional group) was reacted with 35% H_2O_2 in aqueous solution (0.44 mL, 2.50 mmol) in a 4 mL vial.[29] Initially insoluble, PBTGE$_{10}$ dissolved after stirring for 24 h at 37 °C, leaving no insoluble material. Residual H_2O_2 was removed by precipitation with cold diethyl ether, resulting in purified PBSGE$_{10}$. PBSGE$_{10}$: ^{1}H NMR (400 MHz, CD_2Cl_2): δ 7.39–7.29 (m, 50H), 4.29 (s, 20H), 3.85–3.41 (m, 70H), 3.04 (t, 20H).

https://doi.org/10.1021/acs.macromol.4c00949
Macromolecules XXXX, XXX, XXX−XXX

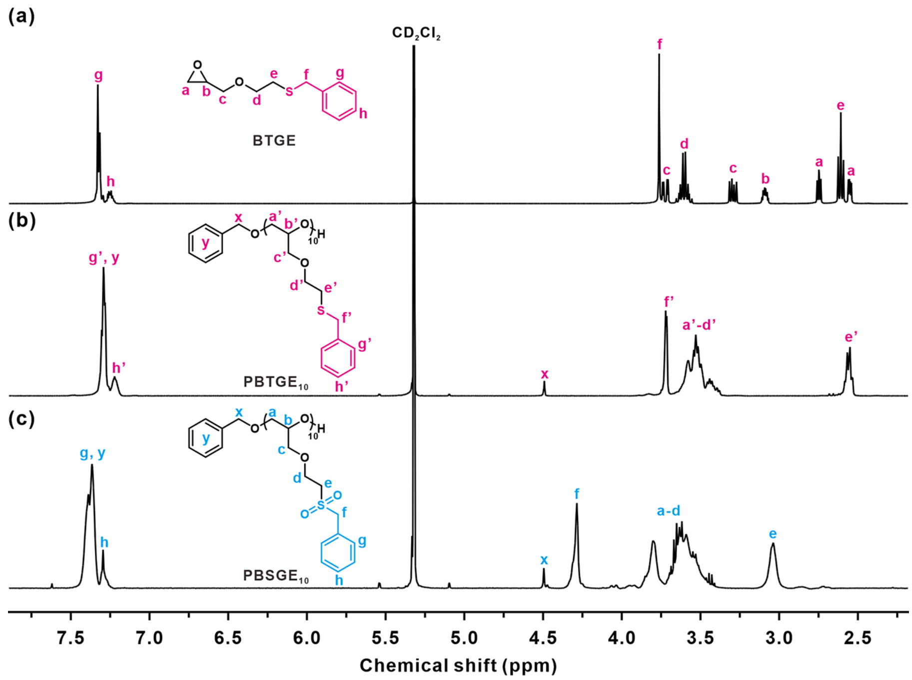

Figure 1. Representative ^{1}H NMR spectra for (a) BTGE monomer, (b) $PBTGE_{10}$ homopolymer (entry 1 in Table 1), and (c) $PBSGE_{10}$ homopolymer (entry 1 in Table S1).

Reductive-Deprotection of PBTGE Homopolymers. In a 4 mL vial, 60 mg of $PBTGE_{10}$ (0.25 mmol of the thioether functional group) was dissolved in neat trifluoroacetic acid (TFA), with the subsequent addition of 2 vol % triisopropylsilane (TIPS) with respect to the TFA.[30] The mixture was incubated for 24 h at 37 °C, then precipitated with cold diethyl ether.

Synthesis of PBTGE-*b*-PEO-*b*-PBTGE ABA Triblock Copolymers. ABA block copolymers were synthesized following procedures outlined in previous research,[31] and initiated using PEO (M_n = 20,000 g mol^{-1}) as the macroinitiator. Next, 3000 mg (0.15 mmol) of PEO was placed into a Schlenk flask under nitrogen, dissolved in 2.0 mL of toluene at 60 °C for 30 min. Subsequently, 0.375 mL of *t*-BuP_4 (0.80 M in *n*-hexane, 0.30 mmol) was added at 40 °C for 30 min. After adding the BTGE monomer (302.52 mg, 1.35 mmol) dropwise, the reaction proceeded for 1 h at 40 °C. An excess of methanol was used to quench the reaction. The mixture was purified by passing it through a basic alumina oxide column with DCM as the eluent. The resulting polymer was dissolved in DCM and precipitated by adding a 20-fold excess hexane. ^{1}H NMR (400 MHz, CD_2Cl_2): δ 7.39−7.13 (d, 40H), 3.96−3.23 (m, 1880H), 2.57 (s, 16 H). ^{13}C NMR (101 MHz, CD_2Cl_2): δ 139.05, 129.69−128.50, 127.41, 71.85−70.64, 37.41, 31.30.

Preparation of Hydrogels and Oxidation-Induced Dissolution Experiments. A $PBTGE_4$-*b*-PEO_{20K}-*b*-$PBTGE_4$ triblock copolymer (40 mg) was dissolved in 0.8 mL of deionized water to form 5 wt % hydrogels. These hydrogels were then equilibrated at 37 °C for 24 h to facilitate homogeneous gelation. Next, the gels were incubated at 37 °C in 100 mM of H_2O_2 (300 μL, 2 equiv with respect to thioether) to evaluate the oxidation-induced dissolution. The transformation of the hydrophobic thioether group into the hydrophilic sulfone group was assessed using ex situ ^{1}H NMR spectroscopy. For this purpose, gel samples were extracted after a designated incubation period, followed by lyophilization.

Rheological Characterization of PBTGE-*b*-PEO-*b*-PBTGE Hydrogels. Oscillatory shear measurements were conducted using an MCR302 rheometer (Anton Paar) equipped with a parallel plate geometry with a 50 mm diameter. To conduct these tests, 5 wt % PBTGE-*b*-PEO-*b*-PBTGE hydrogels were placed on the Peltier plate, maintaining a gap distance of 1 mm. After achieving the required gap height, the edges of the gel were trimmed to ensure complete filling of the geometry. Additionally, the sample stages were encased in water and covered with a solvent trap to maintain the hydration of the hydrogel during the measurements. The oscillatory shear measurements were performed in a frequency range of 0.1−100 rad/s, applying a constant 1% strain at 37 °C.

Oxidation-Induced Model Dye Release Test. A solvent-casting and redispersion method was utilized to load Nile Red in the hydrogel. Briefly, $PBTGE_8$-*b*-PEO_{20K}-*b*-$PBTGE_8$ (250 mg) and Nile Red (100 μg) were dissolved in acetonitrile (5 mL) and the solvent was evaporated using a rotary evaporator. The resulting thin film was redispersed in 5.0 mL of phosphate-buffer saline (PBS 1×, pH 7.4) and incubated at 4 °C overnight. Next, 40 mg of 5 wt % hydrogel was injected into a disposable cuvette, followed by the addition of 2 mL PBS. For the control group, 0.20 mL of PBS was added while 0.10 M H_2O_2 solution (200 μL, 2 equiv with respect to thioether in 20 mg of polymer) was introduced to set the oxidative surrounding. All hydrogels were incubated at 37 °C and the cuvettes were inverted once to mix the sol fraction into the media before measuring the fluorescence intensity (λ_{ex} = 480 nm).

RESULTS AND DISCUSSION

A BTGE monomer was successfully synthesized via a one-step reaction and purified using column chromatography and

Table 1. Characterization of the As-prepared PBTGE Homopolymers and PBTGE-*b*-PEO-*b*-PBTGE Block Copolymers

entry	polymer composition	time (h)	conv.[a] (%)	$M_{n,th}$ (g/mol)	$M_{n,NMR}$[b] (g/mol)	$M_{n,GPC}$[c] (g/mol)	$Đ$[c]	T_g[d] (°C)
1	$PBTGE_{10}$	1	>99	2350	3020	2490	1.10	−37.3
2	$PBTGE_{25}$	2	96.4	5510	6380	4580	1.10	−36.2
3	$PBTGE_{50}$	4	94.3	10,680	10,420	6200	1.11	−34.5
4	$PBTGE_{100}$	12	80.0[e]	18,050	19,850	8140	1.13	−33.2
5	$PBTGE_4$-*b*-PEO_{20K}-*b*-$PBTGE_4$	1	>99	22,010	21,790	21,900	1.11	−37.8, 59.1[f]
6	$PBTGE_6$-*b*-PEO_{20K}-*b*-$PBTGE_6$	1	>99	22,910	22,690	22,980	1.10	−37.4, 58.5[f]
7	$PBTGE_8$-*b*-PEO_{20K}-*b*-$PBTGE_8$	2	>99	23,810	23,580	23,980	1.10	−37.2, 58.1[f]

[a]Calculated from the ^{1}H NMR spectra of the crude mixture. [b]Determined from the ^{1}H NMR spectra of the isolated polymers (CH_2Cl_2, 400 MHz). [c]Measured by GPC (THF, RI signal, PS standard). [d]Determined by DSC at a rate of 10 °C min^{-1}. [e]Reaction conducted in toluene at 25 °C, $[M]_0$ = 2.0 M. [f]T_m of the resulting PBTGE-*b*-PEO-*b*-PBTGE.

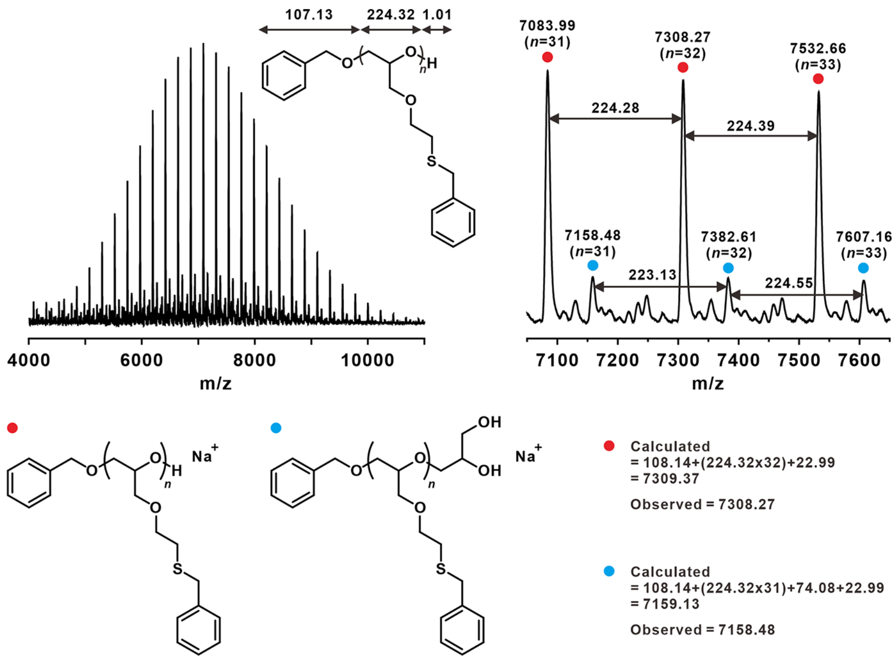

Figure 2. MALDI-ToF mass spectrum of $PBTGE_{50}$ (entry 3 in Table 1). Experimental conditions; reflector positive mode using sodium trifluoroacetate (NaTFA) as an ionization agent and *trans*-2-[3-(4-*tert*-butylphenyl)-2-methyl-2-propenylidene]malononitrile (DCTB) as a matrix.

fractional distillation, producing an isolated yield of 68% (Scheme 1b). The chemical structure of BTGE was confirmed using a range of NMR spectroscopic techniques, including ^{1}H-, ^{13}C NMR, correlation spectroscopy (COSY), heteronuclear single-quantum correlation (HSQC), as well as the electrospray ionization mass spectrum (ESI-MS) (Figures 1a and S2–S5).

Controlled anionic ring-opening polymerization was then performed using benzyl alcohol as the initiator and the organic phosphazene base *t*-BuP_4 at room temperature (Scheme 1c). The highly basic organic superbase *t*-BuP_4 was employed as it enabled the controlled polymerization of the BTGE monomer under mild conditions. The ^{1}H NMR spectra revealed the successful conversion of the monomer to polymer, evidenced by the disappearance of the epoxide peaks (a and b) in the monomer at 3.09, 2.75, and 2.55 ppm and the emergence of peaks at 4.49 and 3.37−3.75 ppm, corresponding to the benzylic protons (*x*) and polyether backbone protons (a'−d'), respectively (Figure 1b). The theoretical number-average molecular weight ($M_{n,NMR}$) and the degree of polymerization (DP) were calculated based on the integral ratio of the polymeric backbone protons to the benzylic protons in the ^{1}H NMR spectra (Figure 1b and Table 1).

The synthesized PBTGE homopolymers were further characterized by ^{1}H- and ^{13}C NMR, gel permeation chromatography (GPC), and matrix-assisted laser desorption/ionization time-of-flight (MALDI-ToF) mass spectrometry (Figures 2, S6 and S7). In particular, MALDI-ToF spectrometry was employed to assess the initiation efficiency and perform an end-group analysis, thereby confirming the controlled polymerization of PBTGE (Figure 2). The spectrum revealed two distributions with a constant interval of 224.32 g mol^{-1}, corresponding to the molar mass of BTGE that demonstrates the successful polymerization. Notably, a prominent peak at 7308.27 g mol^{-1} corresponds to the PBTGE homopolymer, which includes the benzyl alcohol initiator (108.14 g mol^{-1}) and 31 monomer units (224.32 g mol^{-1}) with Na^+ as the counterion. Furthermore, the minor distributions (blue circle) indicated that a single 2-(benzylthio)ethanol group was cleaved during the ionization procedure, producing one glycidol unit per PBTGE chain in accord with previous literature.[32] Consequently, all peaks in the spectrum are attributed to the benzyl alcohol-initiated PBTGE polymers, underscoring the exceptional initiation efficiency. Moreover, the thermal properties of various PBTGE polymers were assessed through differential scanning

https://doi.org/10.1021/acs.macromol.4c00949
Macromolecules XXXX, XXX, XXX−XXX

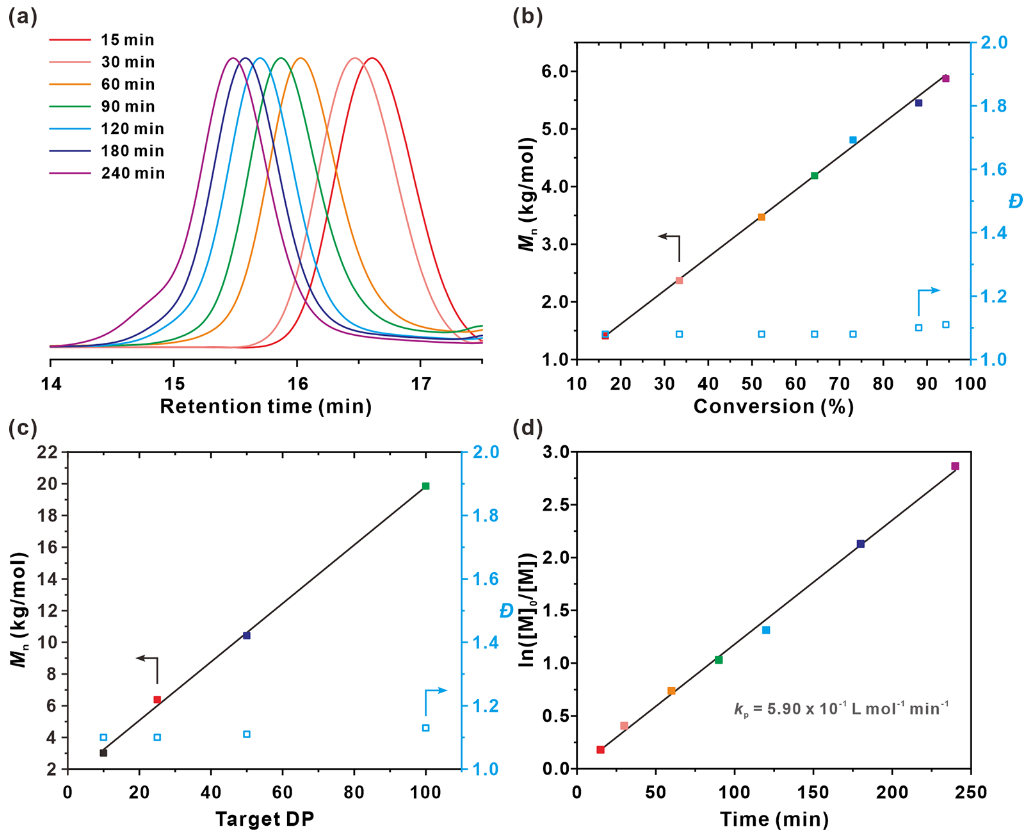

Figure 3. Polymerization kinetics of the $PBTGE_{50}$ (entry 3 in Table 1): (a) GPC chromatograms of $PBTGE_{50}$ sampled at various reaction times using THF as the eluent and PS as the standard. (b,c) Evolution of $M_{n,NMR}$ and molecular weight dispersity ($Đ$) vs (b) monomer conversion and (c) target DP. (d) First-order kinetic curve illustrating the relationship with polymerization time.

calorimetry (DSC) measurements (Figure S8 and Table 1). The glass transition temperature (T_g) increased from −37.3 to −33.2 °C as the DP of the PBTGE increased from 10 to 100.

As illustrated in Table 1, the GPC analysis of the PBTGE homopolymers indicates a monomodal distribution with a narrow dispersity ($Đ$) ranging from 1.10 to 1.13, demonstrating a controllable polymerization. It is noteworthy that the $M_{n,GPC}$ values tend to be slightly lower than the $M_{n,NMR}$ values, possibly due to the high hydrophobicity of the BTGE monomer as similarly observed in other hydrophobic glycidyl ether monomers.[33,34]

To further validate the controlled polymerization of PBTGE, the polymerization kinetics of $PBTGE_{50}$ were investigated using ^1H NMR and GPC at various reaction time (Figure 3). Here, the $PBTGE_{50}$ exhibits a distinct shift toward smaller elution volumes with a lower retention time, indicating the synthesis of polymers with higher molecular weights (Figure 3a). Meanwhile, linear increases in the molar mass ($M_{n,NMR}$) and molecular weight dispersity ($Đ$) as functions of conversion and target DP at low $Đ$ values signify controlled polymerization (Figure 3b,c). Moreover, the linear relationship observed in the plot of $\ln([M]_0/[M]_t)$ vs reaction time suggests a first-order reaction with living characteristics (Figure 3d). Specifically, the polymerization of $BTGE_{50}$ using the t-BuP_4 base system exhibited an accelerated propagation rate (k_p = 5.90 × 10^{-1} L mol^{-1} min^{-1}), exceeding the reactivity of other reported glycidyl ether derivatives, such as ethoxyethyl glycidyl ether (EEGE; 2.23 × 10^{-1} L mol^{-1} min^{-1}), allyl glycidyl ether (AGE; 3.00 × 10^{-1} L mol^{-1} min^{-1}), 4,4-dimethyl-2-oxazoline glycidyl ether (DOGE; 3.66 × 10^{-1} L mol^{-1} min^{-1}), and benzyl glycidyl ether (BnGE; 4.12 × 10^{-1} L mol^{-1} min^{-1}).[34,35] This enhanced reactivity is attributed to the elevated nucleophilicity of the highly polarizable sulfur in the BTGE monomer, which effectively stabilizes the transition state and improves coordination with t-BuP_4H^+, weakening the alkoxide-counterion interaction and facilitating the epoxide ring-opening reaction.[36]

The hydrophobic thioether-containing PBTGE exhibits oxidation-responsive properties, transforming into a hydrophilic sulfone group and leading to the formation of PBSGE upon introduction of hydrogen peroxide (H_2O_2) at 37 °C (Scheme 1c). The conversion of the $PBTGE_{10}$ to $PBSGE_{10}$ was evidenced by the clear downfield shift in the methylene peaks adjacent to sulfur due to the introduction of electron-withdrawing groups (Figure 1c).

The FT-IR spectra of the BTGE, the $PBTGE_{10}$, and the $PBSGE_{10}$, as presented in Figure 4a, show a distinct peak at 1315 cm^{-1} in $PBSGE_{10}$ corresponding to the sulfone moiety, while the peaks related to C−H stretching and bending vibrations remain unchanged. Furthermore, the GPC analysis of PBSGE polymers displayed no noticeable change in retention time, although the $M_{p,GPC}$ value increased marginally due to the presence of the hydrophilic sulfone moiety. This indicates successful oxidation without degradation of the polymer backbone (Figure S9 and Table S1). Meanwhile, DSC analysis of $PBSGE_{10}$ revealed a significant increase in the T_g from −37.3 to 16.8 °C upon oxidation of $PBTGE_{10}$ (Figure S10), attributed to the increased polarity introduced by sulfone moieties in the side chains, thereby suggesting potential intermolecular interactions with the polyether backbone. After

https://doi.org/10.1021/acs.macromol.4c00949
Macromolecules XXXX, XXX, XXX−XXX

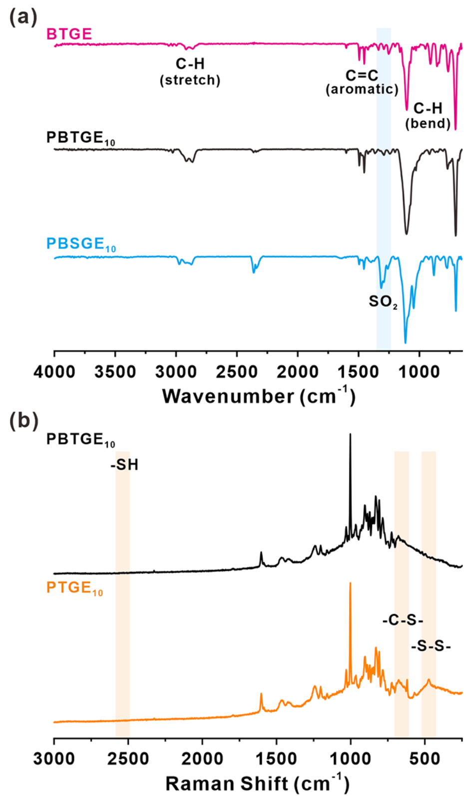

Figure 4. (a) FT-IR spectra of BTGE, $PBTGE_{10}$, and $PBSGE_{10}$ (Table S1). (b) Representative Raman spectra of $PBTGE_{10}$ and $PTGE_{10}$, indicating the presence of sulfone and disulfide groups following deprotection and spontaneous oxidation, respectively.

deprotection, the free thiol groups readily oxidized to form disulfide bonds, followed by thiol−disulfide exchange, resulting in a cross-linked network. Unfortunately, the introduction of dithiothreitol to reduce the cross-linked disulfide group yielded a limited success under the ambient conditions. Consequently, it was limited to analyze the cross-linked structure via conventional methods. Thus, $PBTGE_{10}$ and the deprotected $PTGE_{10}$ were analyzed using Raman spectroscopy (Figure 4b). These results confirm the successful preparation of the desired PTGE polymer, characterized by a distinctive disulfide peak at 476 cm^{-1}, originating from the spontaneous oxidation of the generated free thiol groups.

Subsequently, various PBTGE-*b*-PEO-*b*-PBTGE triblock copolymers with varying proportions of the hydrophobic PBTGE blocks were synthesized by employing poly(ethylene oxide) (PEO; M_n = 20 kDa) as a macroinitiator (entries 5−7 in Table 1). The distinct structural features of the BTGE blocks are characterized through ^{1}H- and ^{13}C NMR spectra (Figures 5a and S11). In addition, GPC analysis indicates that the molecular weight of the triblock copolymers increased relative to that of the PEO in correlation with the increasing number of blocks (Figure S12). Furthermore, DSC analysis provided the thermal properties of the resulting triblock copolymer (Figure S13). Notably, the T_g of the triblock copolymers range from −37.8 to −37.2 °C, aligning with those of the homopolymers. Conversely, the melting temperature (T_m) consistently averages 58.7 °C across all samples, which is attributed to the highly crystalline nature of the PEO midblock.

As shown schematically in Figure 6a, the ABA triblock copolymers, composed of hydrophobic PBTGE end blocks and

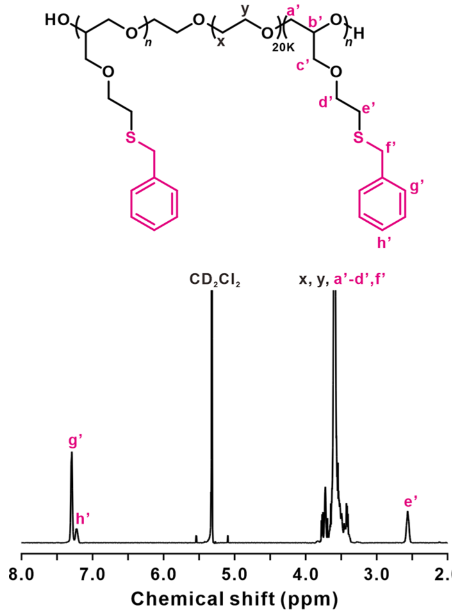

Figure 5. ^{1}H NMR spectrum of $PBTGE_4$-*b*-PEO-*b*-$PBTGE_4$ (entry 5 in Table 1) (400 MHz, CH_2Cl_2).

a central hydrophilic PEO midblock, undergo spontaneous self-assembly in aqueous solution due to hydrophobic interactions. This leads to the formation of micelles with a core−shell structure in which the hydrophobic endblocks aggregate to form the core, and the hydrophilic midblocks arrange into loop-shaped shells on the surface, resembling flower petals. The number of intermicellar bridges increases with the increase in polymer concentration, thus resulting in gel formation.[37,38] Subsequent exposure of these hydrogels to H_2O_2 leads to oxidation of the thioether groups to hydrophilic sulfone groups, inducing gel dissolution by oxidation.

The changes in viscoelastic properties of the 5 wt % $PBTGE_4$-*b*-PEO-*b*-$PBTGE_4$ and $PBTGE_6$-*b*-PEO-*b*-$PBTGE_6$ hydrogels (entries 5 and 6 in Table 1) upon incubation with 100 mM H_2O_2 at 37 °C are evidenced by vial inversion tests (Figure 6b). Here, the $PBTGE_4$-*b*-PEO-*b*-$PBTGE_4$ hydrogel undergoes the transition to a sol state after 12 h and fully dissolves after 36 h. In contrast, the $PBTGE_6$-*b*-PEO-*b*-$PBTGE_6$ hydrogel remains in the gel state for up to 24 h before beginning the transition to a sol state at 36 h. Meanwhile, using the $PBTGE_8$-*b*-PEO-*b*-$PBTGE_8$ results in a delayed transition from gel to sol, occurring over 5 days due to increased hydrophobicity.

Quantitative analysis via ^{1}H NMR elucidated the changes in functional moieties of the $PBTGE_4$-*b*-PEO-*b*-$PBTGE_4$ hydrogel over time (Figure 6c). The thioether peak at 2.50−2.57 ppm gradually decreases, while the sulfoxide (2.57−2.75 ppm) and sulfone (2.75−2.93 ppm) peaks appear at 12 h and increase in intensity thereafter, with polyether backbone peaks (3.23−4.17 ppm) merging, indicating oxidation and transition to a hydrophilic state.[39] Quantitatively, the proportion of thioether groups reduces to 38%, 13%, and 0% at 12, 24, and 36 h, respectively. Notably, the sulfone content, constituting 58%, surpasses that of the sulfoxide at 36 h (Table S2).

Oscillatory shear measurements were performed to unveil the rheological properties of PBTGE-*b*-PEO-*b*-PBTGE hydrogels. A strain sweep was initially conducted to determine a shear strain value that maintained stable linear viscoelastic

https://doi.org/10.1021/acs.macromol.4c00949
Macromolecules XXXX, XXX, XXX−XXX

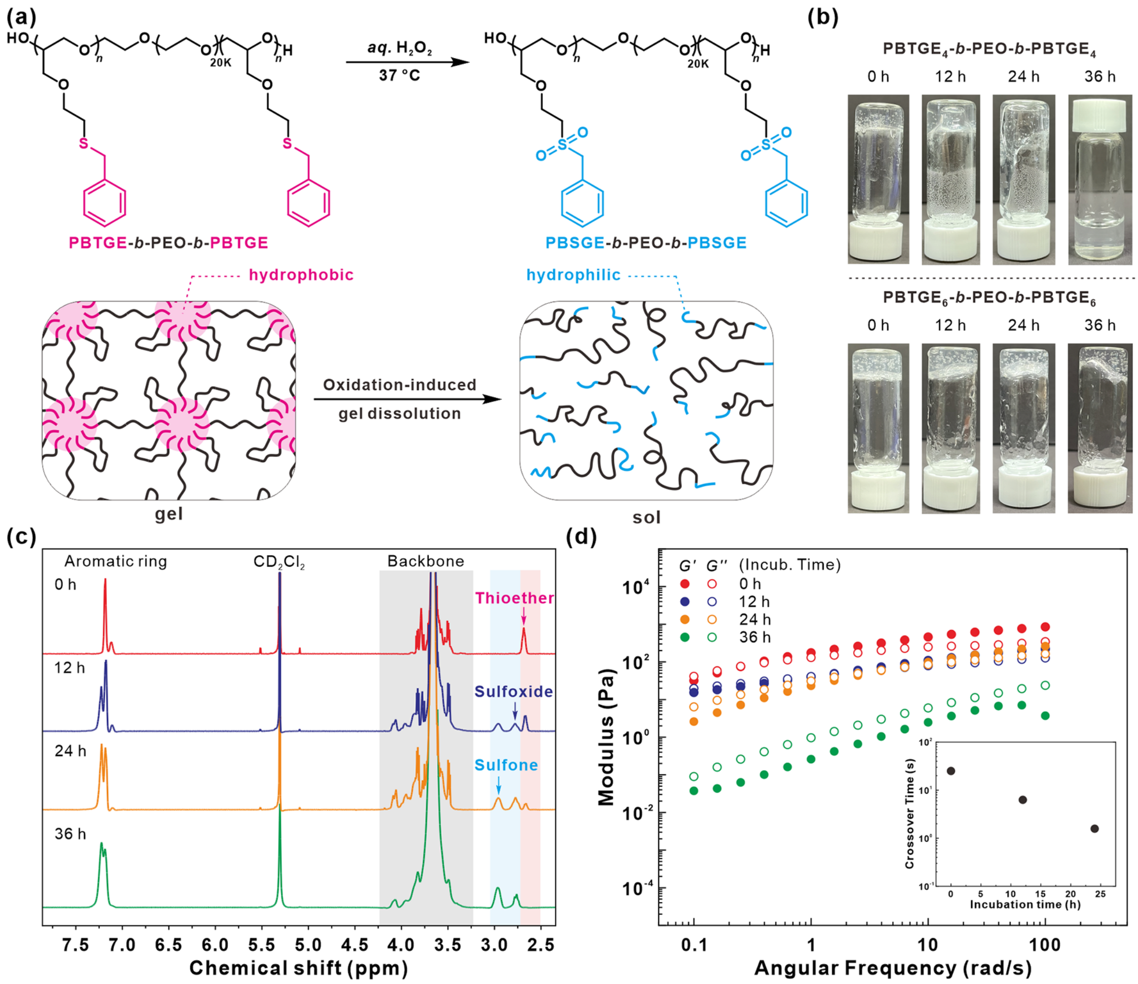

Figure 6. (a) Schematic diagram depicting the disassembly of redox-active triblock hydrogel upon treatment with H_2O_2, leading to a transition from hydrophobic thioether groups to hydrophilic sulfone groups; (b) vial inversion tests for the 5 wt % $PBTGE_4$-*b*-PEO-*b*-$PBTGE_4$ and $PBTGE_6$-*b*-PEO-*b*-$PBTGE_6$ hydrogels (entries 5 and 6 in Table 1), showing oxidation-induced gel dissolution after incubation at 37 °C with 100 mM H_2O_2. (c) Ex situ ^{1}H NMR spectra of $PBTGE_4$-*b*-PEO-*b*-$PBTGE_4$ following incubation with 100 mM H_2O_2 for various durations; (d) frequency sweep measurements of the $PBTGE_4$-*b*-PEO-*b*-$PBTGE_4$ hydrogel. The inset presents the crossover times determined from the intersection frequency of G' and G''.

behavior up to a specified yield strain. Based on this, a constant 1% strain was chosen for further measurements within the linear viscoelastic range. Interestingly, the hydrogels displayed no temperature-responsive behavior within the tested temperature range of 4−37 °C unlike the previously reported hydrogels synthesized from tetrahydropyranyl glycidyl ether and 1-(cyclohexyloxy)ethyl glycidyl ether monomers (Figure S14).[31,40] The viscoelastic properties of the PBTGE-*b*-PEO-*b*-PBTGE hydrogels were influenced by hydrophobic interactions, as evidenced by the frequency-dependent storage modulus (G') and loss modulus (G'') observed during frequency sweep measurements (Figures 6d and S15). At lower frequencies, a predominantly viscous behavior was indicated by a lower G' relative to G''. Conversely, at higher frequencies, G' surpassed G'' and approached the plateau modulus (G), thus suggesting a predominantly elastic behavior. This behavior underscores the gel-to-sol transition of the $PBTGE_4$-*b*-PEO-*b*-$PBTGE_4$ hydrogel at 12 h, achieving a complete sol state after 36 h, in good agreement with the vial inversion results. In addition, the crossover time gradually decreased with prolonged incubation, attributed to enhanced chain dynamics due to oxidation-responsive disassembly (Figure 6d inset).

Remarkably, a time-oxidation superposed master curve for the $PBTGE_4$-*b*-PEO-*b*-$PBTGE_4$ hydrogel was constructed over various incubation times by adjusting the dynamic moduli (Figure S16), akin to the widely employed time−temperature superposition technique.[41,42] This curve revealed that the relaxation behavior of the hydrogel is primarily governed by the degree of oxidation over time, leading to a gradual transition from a hydrophobic to a hydrophilic sulfone core group, which results in predictable degradation of hydrogel. To further underscore its potential in biomedical field, the capability of hydrogel to controlled release system of model hydrophobic molecule was demonstrated (Figure S17). These features promise that it is well-suited for therapeutic applications such as cancer treatment or wound dressing, where high oxidative stress exists and local and sustained drug delivery is required simultaneously.

■ CONCLUSION

In summary, we have successfully demonstrated the synthesis of a benzyl thioether epoxide monomer, BTGE, serving as a

https://doi.org/10.1021/acs.macromol.4c00949
Macromolecules XXXX, XXX, XXX−XXX

versatile building block for developing redox-responsive polyethers and hydrogels. Through controlled anionic ring-opening polymerization, various PBTGE homopolymers and PBTGE-*b*-PEO-*b*-PBTGE triblock copolymers were synthesized with a high degree of with precise control over the polymerization process. The reduction of thioether groups led to the generation of free thiol groups, thereby providing versatility of the polymers. Moreover, these polymers exhibited oxidation-responsive properties, transitioning from hydrophobic to hydrophilic state under oxidative conditions. The utility of the polymers in hydrogel applications was evidenced by a gel-to-sol transition and a controlled release of hydrophobic model molecule under oxidative conditions. This study highlighted the potential of BTGE as a multifunctional monomer for developing advanced materials with redox-responsive properties, paving new avenues for the design of functional materials across various fields.

■ ASSOCIATED CONTENT

Supporting Information

The Supporting Information is available free of charge at https://pubs.acs.org/doi/10.1021/acs.macromol.4c00949.

Experimental procedures and supplemental characterization data, comprising ^{1}H-, ^{13}C-, COSY-, HSQC-NMR, GPC, DSC, and rheological analyses (PDF)

■ AUTHOR INFORMATION

Corresponding Author

Byeong-Su Kim − *Department of Chemistry, Yonsei University, Seoul 03722, Republic of Korea;* orcid.org/0000-0002-6419-3054; Email: bskim19@yonsei.ac.kr

Authors

Ahyun Kim − *Department of Chemistry, Yonsei University, Seoul 03722, Republic of Korea;* orcid.org/0000-0001-9486-8094

Jinsu Baek − *Department of Chemistry, Yonsei University, Seoul 03722, Republic of Korea;* orcid.org/0000-0002-6393-9176

Complete contact information is available at: https://pubs.acs.org/10.1021/acs.macromol.4c00949

Notes

The authors declare no competing financial interest.

■ ACKNOWLEDGMENTS

This work was supported by the National Research Foundation of Korea (NRF-2021R1A2C3004978 and NRF-2021M3H4A1A04092882).

■ REFERENCES

(1) Chen, F.-M.; Liu, X. Advancing Biomaterials of Human Origin for Tissue Engineering. *Prog. Polym. Sci* **2016**, *53*, 86−168.

(2) Kocak, G.; Tuncer, C.; Bütün, V. pH-Responsive Polymers. *Polym. Chem* **2017**, *8*, 144−176.

(3) Ma, P.; Lai, X.; Luo, Z.; Chen, Y.; Loh, X. J.; Ye, E.; Li, Z.; Wu, C.; Wu, Y.-L. Recent Advances in Mechanical Force-Responsive Drug Delivery Systems. *Nanoscale Adv* **2022**, *4*, 3462−3478.

(4) Jochum, F. D.; Theato, P. Temperature- and Light-Responsive Smart Polymer Materials. *Chem. Soc. Rev* **2013**, *42*, 7468−7483.

(5) Mu, J.; Lin, J.; Huang, P.; Chen, X. Development of Endogenous Enzyme-Responsive Nanomaterials for Theranostics. *Chem. Soc. Rev* **2018**, *47*, 5554−5573.

(6) Nakahata, M.; Takashima, Y.; Yamaguchi, H.; Harada, A. Redox-Responsive Self-Healing Materials Formed from Host-Guest Polymers. *Nat. Commun* **2011**, *2*, 511.

(7) Hong, Y.; Kim, J.-M.; Jung, H.; Park, K.; Hong, J.; Choi, S.-H.; Kim, B.-S. Facile Synthesis of Poly(Ethylene Oxide)-Based Self-Healable Dynamic Triblock Copolymer Hydrogels. *Biomacromolecules* **2020**, *21*, 4913−4922.

(8) Fu, X.; Hosta-Rigau, L.; Chandrawati, R.; Cui, J. Multi-Stimuli-Responsive Polymer Particles, Films, and Hydrogels for Drug Delivery. *Chem* **2018**, *4*, 2084−2107.

(9) Sun, H.; Zhong, Z. 100th Anniversary of Macromolecular Science Viewpoint: Biological Stimuli-Sensitive Polymer Prodrugs and Nanoparticles for Tumor-Specific Drug Delivery. *ACS Macro Lett* **2020**, *9*, 1292−1302.

(10) Hu, L.; Zhang, Q.; Li, X.; Serpe, M. J. Stimuli-Responsive Polymers for Sensing and Actuation. *Mater. Horiz* **2019**, *6*, 1774−1793.

(11) Huo, M.; Yuan, J.; Tao, L.; Wei, Y. Redox-Responsive Polymers for Drug Delivery: From Molecular Design to Applications. *Polym. Chem* **2014**, *5*, 1519−1528.

(12) Kim, S.; Chae, J.-B.; Kim, D.; Park, C.-W.; Sim, Y.; Lee, H.; Park, G.; Lee, J.; Hong, S.; Jana, B.; Kim, C.; Chung, H.; Ryu, J.-H. Supramolecular Senolytics via Intracellular Oligomerization of Peptides in Response to Elevated Reactive Oxygen Species Levels in Aging Cells. *J. Am. Chem. Soc* **2023**, *145*, 21991−22008.

(13) Chen, M.; Hu, J.; Wang, L.; Li, Y.; Zhu, C.; Chen, C.; Shi, M.; Ju, Z.; Cao, X.; Zhang, Z. Targeted and Redox-Responsive Drug Delivery Systems Based on Carbonic Anhydrase IX-Decorated Mesoporous Silica Nanoparticles for Cancer Therapy. *Sci. Rep* **2020**, *10*, 14447.

(14) Yang, B.; Chen, Y.; Shi, J. Reactive Oxygen Species (ROS)-Based Nanomedicine. *Chem. Rev* **2019**, *119*, 4881−4985.

(15) Kim, Y. E.; Kim, J. ROS-Scavenging Therapeutic Hydrogels for Modulation of the Inflammatory Response. *ACS Appl. Mater. Interfaces* **2022**, *14*, 23002−23021.

(16) Criado-Gonzalez, M.; Mecerreyes, D. Thioether-Based ROS Responsive Polymers for Biomedical Applications. *J. Mater. Chem. B* **2022**, *10*, 7206−7221.

(17) Shim, M. S.; Xia, Y. A Reactive Oxygen Species (ROS)-Responsive Polymer for Safe, Efficient, and Targeted Gene Delivery in Cancer Cells. *Angew. Chem., Int. Ed* **2013**, *52*, 6926−6929.

(18) Ge, C.; Zhu, J.; Wu, G.; Ye, H.; Lu, H.; Yin, L. ROS-Responsive Selenopolypeptide Micelles: Preparation, Characterization, and Controlled Drug Release. *Biomacromolecules* **2022**, *23*, 2647−2654.

(19) Ma, N.; Li, Y.; Xu, H.; Wang, Z.; Zhang, X. Dual Redox Responsive Assemblies Formed from Diselenide Block Copolymers. *J. Am. Chem. Soc* **2010**, *132*, 442−443.

(20) de Gracia Lux, C.; Joshi-Barr, S.; Nguyen, T.; Mahmoud, E.; Schopf, E.; Fomina, N.; Almutairi, A. Biocompatible Polymeric Nanoparticles Degrade and Release Cargo in Response to Biologically Relevant Levels of Hydrogen Peroxide. *J. Am. Chem. Soc* **2012**, *134*, 15758−15764.

(21) Gupta, M. K.; Lee, S. H.; Crowder, S. W.; Wang, X.; Hofmeister, L. H.; Nelson, C. E.; Bellan, L. M.; Duvall, C. L.; Sung, H.-J. Oligoproline-Derived Nanocarrier for Dual Stimuli-Responsive Gene Delivery. *J. Mater. Chem. B* **2015**, *3*, 7271−7280.

(22) Poetker, D. M.; Reh, D. D. A Comprehensive Review of the Adverse Effects of Systemic Corticosteroids. *Otolaryngol. Clin. N. Am* **2010**, *43*, 753−768.

(23) Hu, B.; Lian, Z.; Zhou, Z.; Shi, L.; Yu, Z. Reactive Oxygen Species-Responsive Adaptable Self-Assembly of Peptides toward Advanced Biomaterials. *ACS Appl. Bio Mater* **2020**, *3*, 5529−5551.

(24) Sarapas, J. M.; Tew, G. N. Thiol-Ene Step-Growth as a Versatile Route to Functional Polymers. *Angew. Chem., Int. Ed* **2016**, *55*, 15860−15863.

(25) Yu, S.; Wang, C.; Yu, J.; Wang, J.; Lu, Y.; Zhang, Y.; Zhang, X.; Hu, Q.; Sun, W.; He, C.; Chen, X.; Gu, Z. Injectable Bioresponsive Gel Depot for Enhanced Immune Checkpoint Blockade. *Adv. Mater* **2018**, *30* (28), 1801527.

(26) Kim, E.-J.; Bhuniya, S.; Lee, H.; Kim, H. M.; Cheong, C.; Maiti, S.; Hong, K. S.; Kim, J. S. An Activatable Prodrug for the Treatment of Metastatic Tumors. *J. Am. Chem. Soc* **2014**, *136*, 13888−13894.

(27) Son, S.; Shin, E.; Kim, B.-S. Redox-Degradable Biocompatible Hyperbranched Polyglycerols: Synthesis, Copolymerization Kinetics, Degradation, and Biocompatibility. *Macromolecules* **2015**, *48*, 600−609.

(28) Herzberger, J.; Fischer, K.; Leibig, D.; Bros, M.; Thiermann, R.; Frey, H. Oxidation-Responsive and "Clickable" Poly(Ethylene Glycol) via Copolymerization of 2-(Methylthio)Ethyl Glycidyl Ether. *J. Am. Chem. Soc* **2016**, *138*, 9212−9223.

(29) Sarapas, J. M.; Tew, G. N. Poly(Ether-Thioethers) by Thiol-Ene Click and Their Oxidized Analogues as Lithium Polymer Electrolytes. *Macromolecules* **2016**, *49*, 1154−1162.

(30) Ste Marie, E. J.; Hondal, R. J. Reduction of Cysteine-*S*-Protecting Groups by Triisopropylsilane. *J. Pept. Sci* **2018**, *24*, No. e3130.

(31) Baek, J.; Kim, S.; Son, I.; Choi, S.-H.; Kim, B.-S. Hydrolysis-Driven Viscoelastic Transition in Triblock Copolyether Hydrogels with Acetal Pendants. *ACS Macro Lett* **2021**, *10*, 1080−1087.

(32) Schüttner, S.; Krappel, M.; Koziol, M.; Marquart, L.; Schneider, I.; Sottmann, T.; Frey, H. Anionic Ring-Opening Copolymerization of Farnesyl Glycidyl Ether: Fast Access to Terpenoid-Derived Amphiphilic Polyether Architectures. *Macromolecules* **2023**, *56*, 6928−6940.

(33) Song, J.; Hwang, E.; Lee, Y.; Palanikumar, L.; Choi, S.-H.; Ryu, J.-H.; Kim, B.-S. Tailorable Degradation of pH-Responsive All Polyether Micelles via Copolymerisation with Varying Acetal Groups. *Polym. Chem* **2019**, *10*, 582−592.

(34) Park, J.; Yu, Y.; Lee, J. W.; Kim, B.-S. Anionic Ring-Opening Polymerization of a Functional Epoxide Monomer with an Oxazoline Protecting Group for the Synthesis of Polyethers with Carboxylic Acid Pendants. *Macromolecules* **2022**, *55*, 5448−5458.

(35) Puchelle, V.; Du, H.; Illy, N.; Guégan, P. Polymerization of Epoxide Monomers Promoted by *t*BuP$_4$ Phosphazene Base: A Comparative Study of Kinetic Behavior. *Polym. Chem* **2020**, *11* (21), 3585−3592.

(36) Lee, B. F.; Wolffs, M.; Delaney, K. T.; Sprafke, J. K.; Leibfarth, F. A.; Hawker, C. J.; Lynd, N. A. Reactivity Ratios and Mechanistic Insight for Anionic Ring-Opening Copolymerization of Epoxides. *Macromolecules* **2012**, *45*, 3722−3731.

(37) Honda, S.; Yamamoto, T.; Tezuka, Y. Topology-Directed Control on Thermal Stability: Micelles Formed from Linear and Cyclized Amphiphilic Block Copolymers. *J. Am. Chem. Soc* **2010**, *132*, 10251−10253.

(38) Jung, H.; Gang, S.-E.; Kim, J.-M.; Heo, T.-Y.; Lee, S.; Shin, E.; Kim, B.-S.; Choi, S.-H. Regulating Dynamics of Polyether-Based Triblock Copolymer Hydrogels by End-Block Hydrophobicity. *Macromolecules* **2020**, *53*, 10339−10348.

(39) Razavi-Esfali, M.; Habets, T.; Siragusa, F.; Grignard, B.; Sardon, H.; Detrembleur, C. Design of Functional Isocyanate-Free Poly-(oxazolidone)s Under Mild Conditions. *Polym. Chem* **2024**, *15*, 1962−1974.

(40) Son, I.; Lee, Y.; Baek, J.; Park, M.; Han, D.; Min, S. K.; Lee, D.; Kim, B.-S. pH-Responsive Amphiphilic Polyether Micelles with Superior Stability for Smart Drug Delivery. *Biomacromolecules* **2021**, *22*, 2043−2056.

(41) Sun, J.; Schiffman, J. D.; Perry, S. L. Linear Viscoelasticity and Time-Alcohol Superposition of Chitosan/Hyaluronic Acid Complex Coacervates. *ACS Appl. Polym. Mater* **2022**, *4*, 1617−1625.

(42) Suarez-Martinez, P. C.; Batys, P.; Sammalkorpi, M.; Lutkenhaus, J. L. Time-Temperature and Time-Water Superposition Principles Applied to Poly(Allylamine)/Poly(Acrylic Acid) Complexes. *Macromolecules* **2019**, *52*, 3066−3074.

https://doi.org/10.1021/acs.macromol.4c00949
Macromolecules XXXX, XXX, XXX−XXX